EXPERIMENTAL STUDY OF MANEUVERABILITY HYDRODYNAMICS OF A MINI-UNDERWATER VEHICLE

Ni GAO[1], Shuzheng SUN[2*]

The Mini-Underwater Vehicles (MUV) are widely used for its small displacement and easily to be controlled. Because of the problems of low propelling efficiency, the motions and the bow up state of the MUV are easily to be influenced by the fluid during the sailing near the free surface. Therefore, the hydrodynamic performance of MUV should be investigated to control the motions of MUV more efficient. The hydrodynamic performances of a MUV near the free surface are investigated experimentally in this paper. The horizontal cycling tunnel and the vertical planar motion mechanism (VPMM) are used to measure some important hydrodynamic coefficients of the MUV. The model test data can provide the validation and verification for the numerical calculation of hydrodynamic coefficients, and also the direction for the numerical maneuver simulation near the free surface of the MUV.

Keywords: MUV, near free surface, VPMM, experiment

1. Introduction

There are abundant resources in the ocean. With the development of human society and the increasing scarcity of land resources, the abundant mineral resources and biological resources in the ocean have been paid more and more attention. The underwater vehicles get fast development in the process of ocean resource exploration [1]. MUV has many unique advantages, such as low noise, low resistance, good stealth performance, low construction cost, easy to mass production and so on. It has a good application prospect in military and civilian fields [2-3].

[1]School of Water Conservancy and Civil Engineering, Northeast Agricultural University, Harbin 150030, China
[2]College of Shipbuilding Engineering, Harbin Engineering University, Harbin 150001, China, e-mail: sunshuzheng@hrbeu.edu.cn

MUV works in deep water most of the time, but when it is deployed and recovered from the platform and floats for navigation and positioning after a period of time, the MUV may be affected by the free surface. When the MUV navigates in the depth range which is significantly affected by the free surface, we call it near the free surface. Because of its small size and light weight, the MUV is easily to be disturbed by wind, wave, current and free surface. The study of its hydrodynamic performance near the free surface can help the MUV adapt to the near free surface flow field, effectively maintain its own state of navigation, and achieve accurate control in the water.

The flow field of MUV becomes more complex when it gets close to the free surface, which makes the numerical calculation difficult [4-5]. In order to obtain the hydrodynamic coefficientsfor MUV motion equations, resistance, manoeuvrability, heave and pitch near the water surface accurately and provide experimental verification for numerical calculation, some important hydrodynamic coefficients of the MUV with multiple depths are measured by using horizontal circulating tunnel and Vertical Planar Motion Mechanism (VPMM), and part of the hydrodynamic force is obtained [6-8].Qi, Miao and Wan calculated the hydrodynamic derivatives of an autonomous and remotely-operated vehicle (ARV) at different drift and attack angles using open source CFD code OpenFOAM [9]. Kolodziejczyk presents a method of determination of transient hydrodynamic coefficients for the robotic arm, based on previously established time-dependent hydrodynamic load which can be obtained either from experiments or numerical simulations [10]. Avila, Nishimoto, Sampaio, and Adamowski carried out the experiment to get the hydrodynamic coefficients of an open-frame underwater vehicles using a planar motion mechanism [11].

2. Setup of the experiment

2.1 Parameters of the measurement instruments

The test was carried out in a horizontal circulating tunnel of Harbin Engineering University. The main parameters of the tunnel are as follows: the main scale of the tunnel is 17.3m×6m×2.88m, the size of the working part is

7m×1.7m×1.5m, and the max velocity is 4.0m/s. The motion modes of the MUV such as heave and pitch are realized by the VPMM which is shown in Figure 2, the main parameters are: heave amplitude 0.04 m, angle of attack 0-20 degree, oscillation period 1-5 s, frequency 0.2-1 Hz, span of two rods 0.35-1.15 M. The force of the model is measured by the six component force sensor[12]. The measuring range and accuracy of the force and moment sensor is ±500N and ±100N.m with the sensitivity of 0.3%.

Fig.1. Horizontal cycling tunnel

Fig.2. Vertical planar motion mechanism

2.2 Setup of the testing model

The weight of the model is W=37kg, the total length is L=1.46m, the diameter is$D$=214mm. The four flat rudders symmetrically distributed in the stern, the thickness is t=1mm. The force measurement center of the model is 637mm from the bow. The center of gravity of the model is G=661.089mm from the bow. The longitudinal moment of inertia of the model is $I_{yy} = 5.338 kg.m^2$.

The displacement of the MUV model is set to the same as the real one to meet the weight and the longitudinal moment of inertia similarity. The model-to-ship ratio is 1:1. The above weight and moment of inertia are the value including the internal water in the model. The depth of the model h is h/D=1.5, h/D =2.5 and h/D =3.5, respectively. Figure 3 shows the experimental model of the MUV. The sketch of the coordinate system and the model installation is shown in Figure 4.

Fig.3. Testing model of MUV

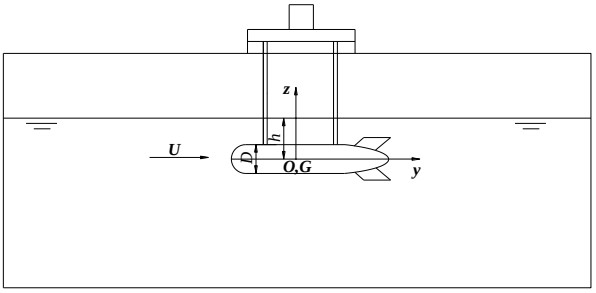

Fig.4. Sketch of the model and the coordinate system

3. Experiment procedure and data analysis

3.1 Test of heading sailing

The hydrodynamic performance of the MUV model is studied experimentally. The longitudinal resistance of the model R=Fy, the vertical force Fz and the trim moment Mx at different velocities (U) caused by the disturbance of the free surface are measured in the heading sailing test. The free surface is

disturbed due to eigen wave induced by the MUV model, at near free surface, and no other excitation sources are considered. The results are shown in Figures 5-7.

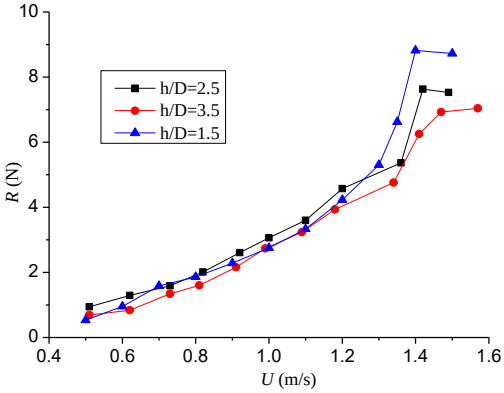

Fig. 5. Resistance of the model

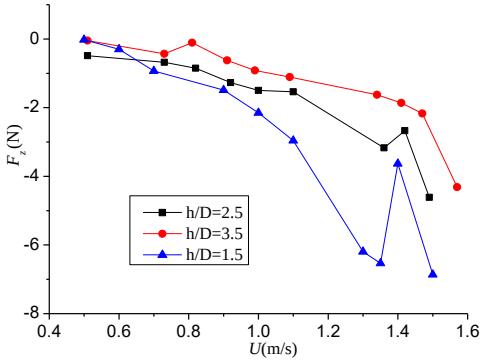

Fig.6. Vertical force of the model

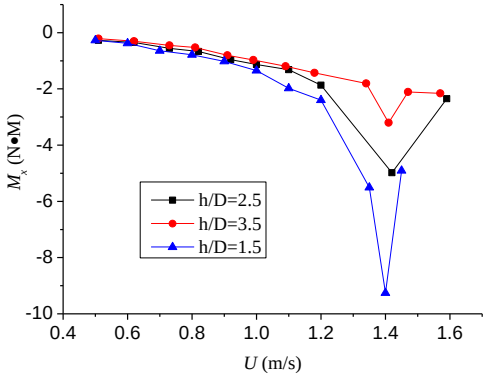

Fig.7. Longitudinal moment of the model

From Figures 5-7, it can be seen that with the decrease of submergence depth, the resistance of the submersible increases, especially when the inflow velocity exceeds 1.0m/s. When the inflow velocity is 1.4m/s, the resistance peak appears. At this velocity, the resistance increases obviously, the vertical force decreases, and the trim moment increases. This phenomenon is mainly caused by wave-making of the model. Since the wave-making resistance increases with the velocity and the action point of lift tends to the stern of the model, the trim moment may get larger as the velocity increases.

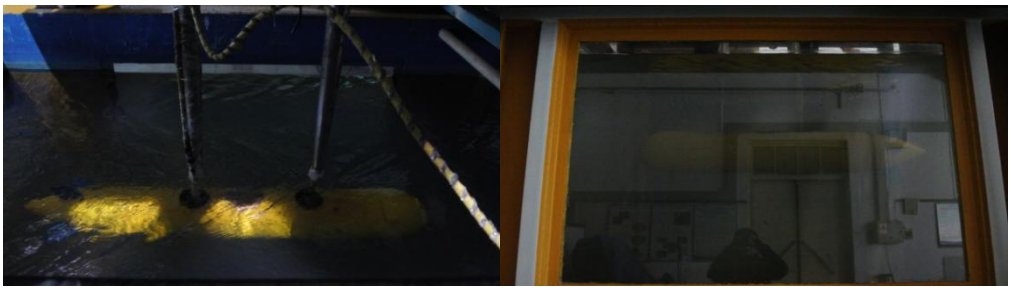

(a) h/D=1.5, U=0.5m/s

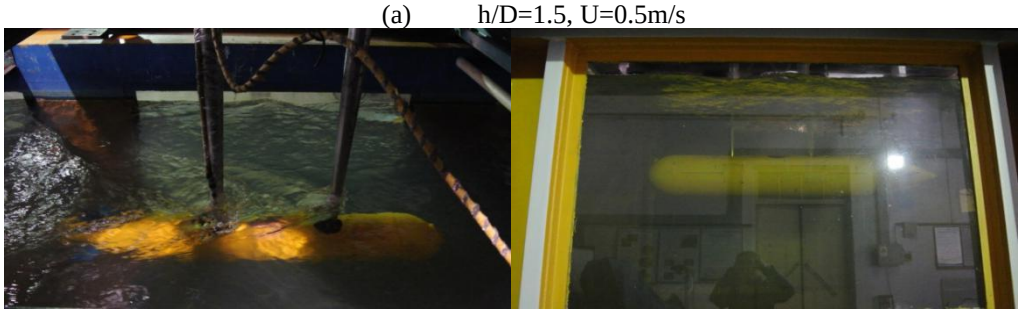

(b) h/D=1.5, U=0.9m/s

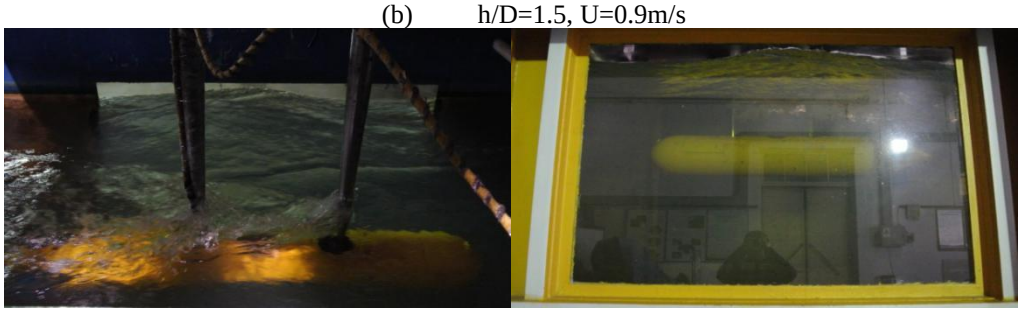

(c) h/D=1.5, U=1.4m/s

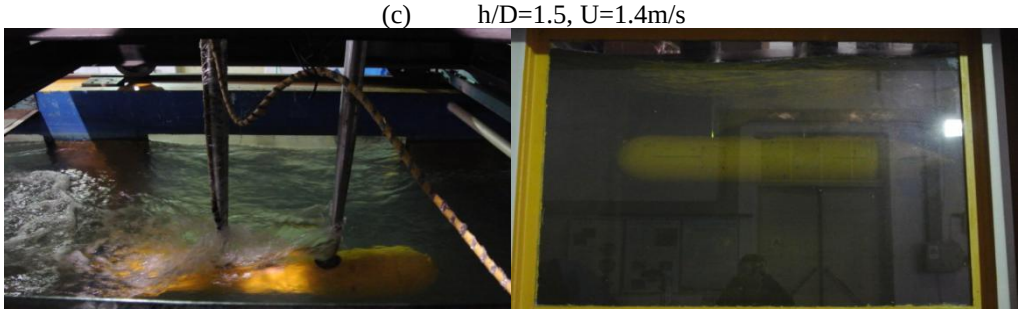

(d) h/D=1.5, U=1.6m/s

Fig. 8.Wave pattern of the free surface at different velocities for h/D=1.5

When h/D=1.5, the wave-pattern of the free surface of the corresponding test model changes with the velocity as shown in Figure 8. When the incoming velocity is 1.4m/s, an obvious wave peak appears on the middle of the model, which also verifies that the peak resistance appears at this velocity. So the MVU should avoid sailing at the speed of about 1.4m/s as far as possible.

3.2 Test of horizontal oblique sailing

The model is rotated so that its mid longitudinal section is at an angle β (drift angle) with the center line of the tunnel. Because of the existence of drift angle β, the model moves in a uniform straight line along the Gx axis and has a lateral disturbance velocity. The drift angle varies from -10° to +10°, and the interval is 2°. The lateral forceFxand yaw momentMz can be measured by the six component sensor. The hydrodynamic forces generated by the oblique sailing of the model at three depths are measured. The test results of lateral force and yaw moment are shown in Figures 9-11.

The test results show that the test results of oblique sailing are almost symmetrical from -10° to 10°. The lateral force and yaw moment at three depths are very close and have good repeatability. It can be concluded that the free surface has little influence on the horizontal oblique sailing. In the test, the yaw moment reaches its peak value at +4° and – 4° respectively, and then decreases gradually. The yaw moment approaches zero when the drift angle is – 10°.

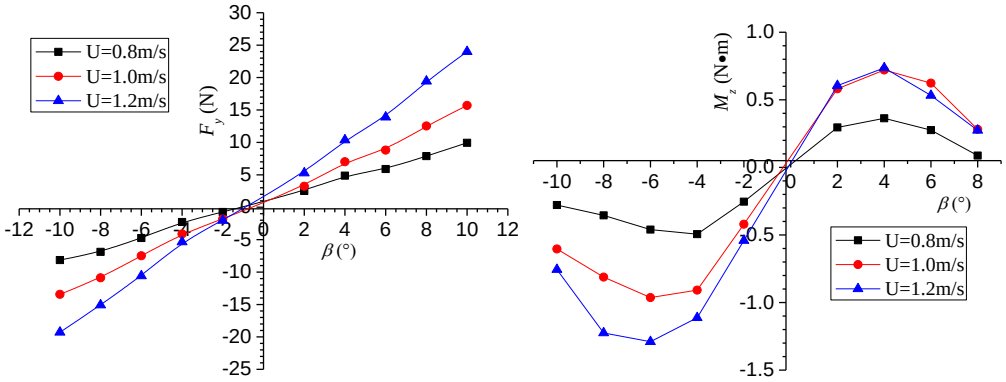

Fig.9. Lateral force and yaw moment as h/D =1.5

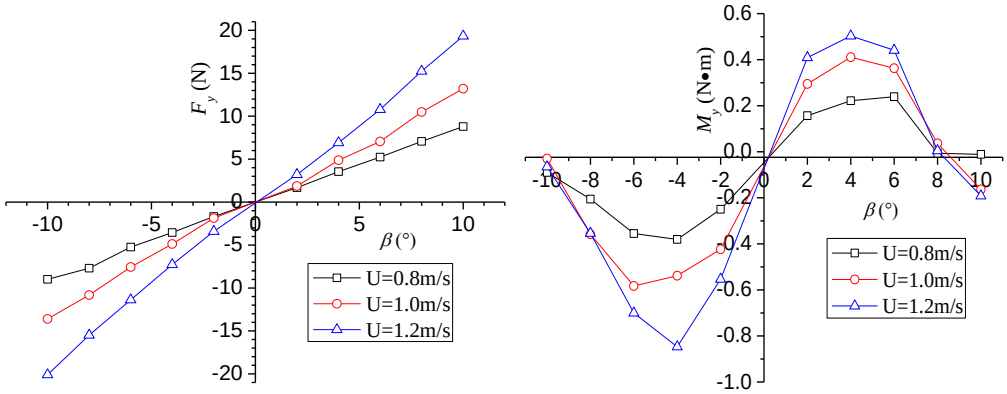

Fig.10. Lateral force and yaw moment as h/D =2.5

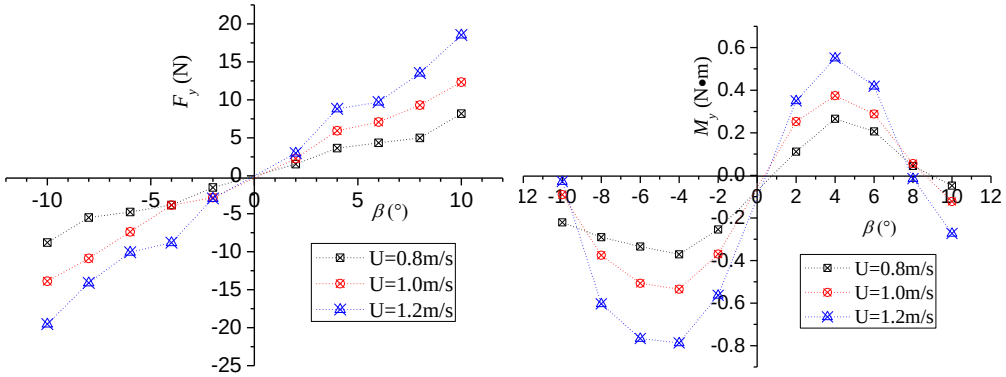

Fig.11. Lateral force and yaw moment as h/D =3.5

3.3 Test of heave and pitching motions

The purpose of the pure heave motion test is to measure the vertical velocity and acceleration hydrodynamic coefficients of the model $Z'_w, Z'_{\dot{w}}, M'_w, M'_{\dot{w}}$. The pure pitch oscillation motion test of the model is to measure the angular velocity and the angular acceleration coefficients in vertical plane $Z'_q, Z'_{\dot{q}}, M'_q, M'_{\dot{q}}$.

The forces and moments measured by the pure heave motion test measuring system include three parts: the fluid inertial forces (moments) in phase with the strut oscillation (displacement); the damping moments orthogonal to the strut oscillation phase; and the constant parts (i.e. zero lift and zero moment). Here the subscript in is used to represent the in-phase component, out is used to represent the orthogonal component. In the experiment, the heave amplitude A = 0.04m, the incoming velocity is 0.8m/s and 1.1m/s, respectively. The force and

moment of the model heave motion are measured at 9 frequencies of 0.1Hz, 0.15Hz, 0.2Hz, 0.25Hz, 0.3Hz, 0.35Hz, 0.4Hz, 0.45Hz, and 0.5Hz. The $Z'_{\dot{w}}$, $M'_{\dot{w}}$, Z'_{w}, of the model can be obtained according to the linearization of different transverse coordinates, such as Z_{in} is the linear function of $a\omega^2$. The linearized results of h/D = 1.5 is shown in Figure 12. Table 1 shows the dimensionless hydrodynamic coefficients of the model with different depths. Table 2 shows the variation of the hydrodynamic coefficients with respect to h/D =1.5 and 2.5 with respect to h/D =3.5.

The forces and moments of heave and pitch motion of the model are as follows:

$$\begin{cases} F_1+F_2=a\omega^2(Z_{\dot{\omega}}-m)\sin\omega t-(a\omega Z_{\omega})\cos\omega t-Z_0 \\ (F_2-F_1)l_0=a\omega^2(M_{\dot{\omega}}+m\dot{x}_G)\sin\omega t-(a\omega M_{\omega})\cos\omega t-M_0 \\ F_1+F_2=\theta_0\omega^2(Z_{\dot{q}}+mx_G)\sin\omega t-\theta_0\omega(Z_q+mV)\cos\omega t-Z_0 \\ (F_2-F_1)l_0=\theta_0\left[\omega^2(M_{\dot{q}}-I_y)+mgh\right]\sin\omega t+\theta_0\omega(mx_GV-M_q)\cos\omega t-M_0 \end{cases} \quad (1)$$

And the forces and moments of the pure heave and pitch motion should be expressed as:

$$\begin{cases} F_1+F_2=Z_{in}\sin\omega t+Z_{out}\cos\omega t+Z_c \\ (F_2-F_1)l_0=M_{in}\sin\omega t+M_{out}\cos\omega t+M_c \\ F_1+F_2=Z_{in}\sin\omega t+Z_{out}\cos\omega t+Z_c \\ (F_2-F_1)l_0=M_{in}\sin\omega t+M_{out}\cos\omega t+M_c \end{cases} \quad (2)$$

where

$$\begin{cases} Z_{in}=a\omega^2(Z_{\dot{\omega}}-m) \\ Z_{out}=-a\omega Z_{\omega} \\ Z_c=-Z_0 \\ M_{in}=a\omega^2(M_{\dot{\omega}}+mx_G) \\ M_{out}=-a\omega M_{\omega} \\ M_c=-M_0 \end{cases} \text{ and } \begin{cases} Z_{in}=\theta_0\omega^2(mx_G+Z_{\dot{q}}) \\ Z_{out}=-\theta_0\omega(Z_q+mV) \\ Z_c=-Z_0 \\ M_{in}=\theta_0\left[\omega^2(M_{\dot{q}}-I_y)+mgh\right] \\ M_{out}=\theta_0\omega(mVx_G-M_q) \\ M_c=-M_0 \end{cases}$$

$$\text{then} \quad \begin{cases} Z_w = \dfrac{-Z_{out}}{a\omega} \\ Z_{\dot{w}} = \dfrac{Z_{in}}{a\omega^2} + m \\ M_w = \dfrac{-M_{out}}{a\omega} \\ M_{\dot{w}} = \dfrac{M_{in}}{a\omega^2} - mx_G \end{cases} \quad \text{and} \quad \begin{cases} Z_{\dot{q}} = \dfrac{Z_{in}}{\theta_0\omega^2} - mx_G \\ Z_q = -\dfrac{Z_{out}}{\theta_0\omega} - mV \\ M_{\dot{q}} = \dfrac{M_{in}}{\theta_0\omega^2} + I_y - \dfrac{mgh}{\omega^2} \\ M_q = -\dfrac{M_{out}}{\theta_0} + mVx_G \end{cases} \tag{3}$$

and then the dimensionless hydrodynamic coefficients can be calculated by:

$$Z = Z' \cdot \frac{1}{2}\rho U^2 L^2$$
$$M = M' \cdot \frac{1}{2}\rho U^2 L^3 \tag{4}$$

In the pure pitch motion test, the angular amplitude θ is 0.3rad, the inflow velocity is 0.8 m/s and 1.1 m/s, and the frequencies are 0.2 Hz, 0.25 Hz, 0.3 Hz, 0.35 Hz, 0.4 Hz and 0.45 Hz, respectively. The linear results of h/D=1.5 is shown in Figure 13. Table 3 shows the dimensionless hydrodynamic coefficients of submersibles at different depths. Table 4 shows the variation of the hydrodynamic coefficients with respect to h/D=3.5 obtained at depths h/D=1.5 and h/D=2.5.

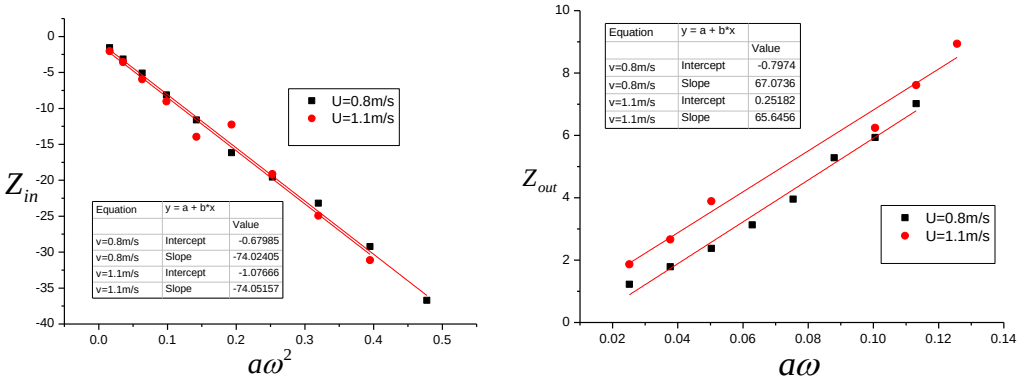

(a) The curve of the same direction force (b) The curve of the orthogonal force

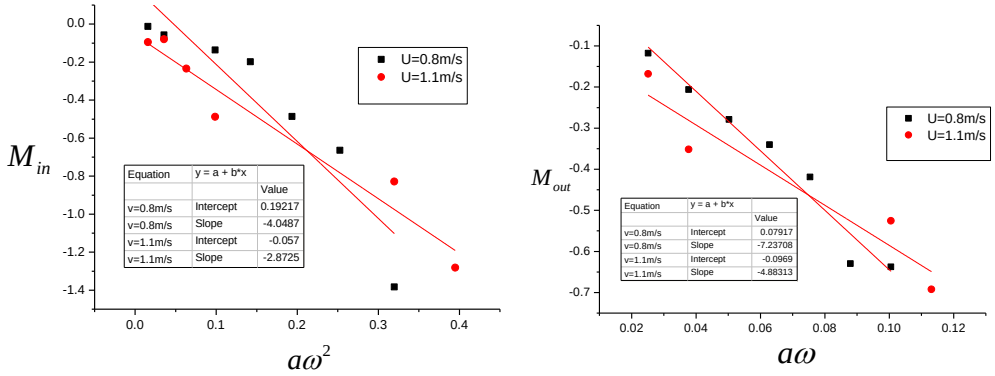

(c) The curve of the same direction moment (d) The curve of the orthogonal moment

Fig.12. The calculation curves of $Z'_{\dot{w}}, M'_{\dot{w}}, Z'_{w}$ and M'_{w} as h/D=1.5

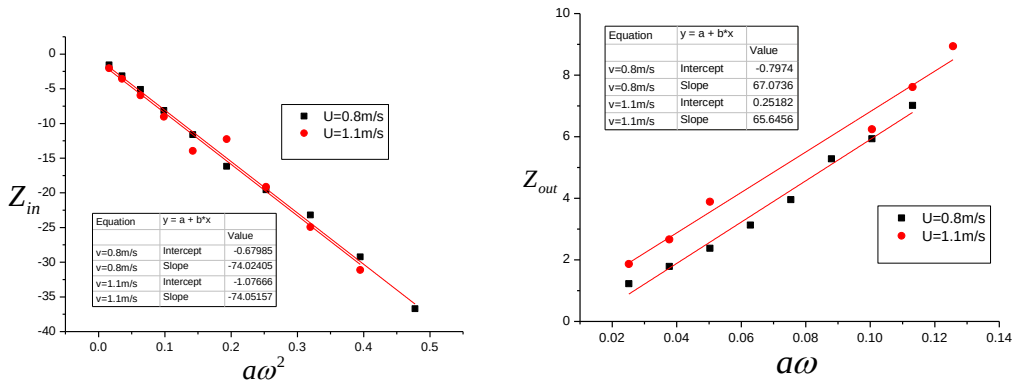

(a) The curve of the same direction force (b) The curve of the orthogonal force

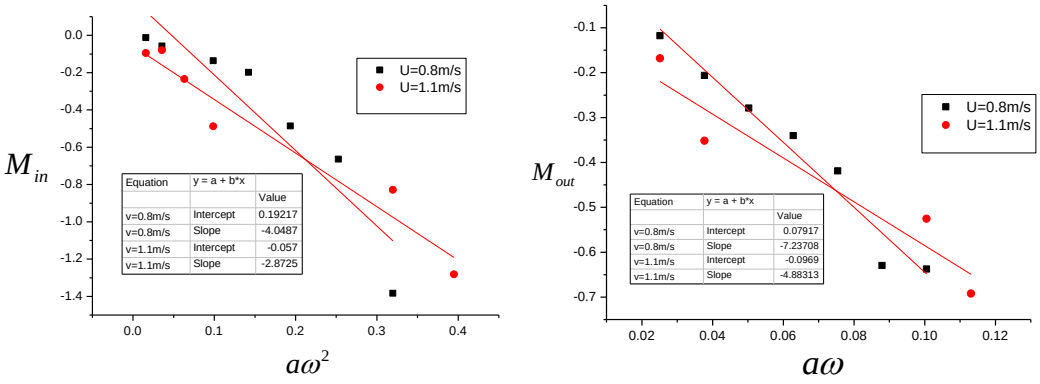

(c) The curve of the same direction moment (d) The curve of the orthogonal moment

Fig.13. The calculation curves of Z'_{q}, $Z'_{\dot{q}}$, M'_{q} and $M'_{\dot{q}}$ as h/D=1.5

Table 1

Model test results of $Z'_{\dot{w}}$, $M'_{\dot{w}}$, Z'_{w} and M'_{w} at different depth

h/D	$Z'_{\dot{w}}$	Z'_{w}	$M'_{\dot{w}}$	M'_{w}
1.5	-0.0238	-0.06733	-0.00113	0.004333
2.5	-0.02524	-0.05109	-0.00044	0.003377
3.5	-0.02509	-0.05126	-0.00047	0.002387

Table 2

Relative changes of $Z'_{\dot{w}}$, $M'_{\dot{w}}$, Z'_{w}, M'_{w} as h/D=1.5, 2.5 compared with h/D=3.5

h/D	$Z'_{\dot{w}}$	Z'_{w}	$M'_{\dot{w}}$	M'_{w}
1.5	-5.14%	31.35%	140.43%	81.52%
2.5	0.60%	-0.33%	-6.38%	41.47%

Table 3

Model test results of Z'_{q}, $Z'_{\dot{q}}$, M'_{q} and $M'_{\dot{q}}$ at different depth

h/D	$Z'_{\dot{q}}$	Z'_{q}	$M'_{\dot{q}}$	M'_{q}
1.5	-0.0061	-0.042294	0.003314	-0.01282
2.5	-0.00696	-0.040417	0.003171	-0.01272
3.5	-0.00716	-0.0396	0.003015	-0.01111

Table 4

Relative changes of Z'_{q}, $Z'_{\dot{q}}$, M'_{q} and $M'_{\dot{q}}$ as h/D=1.5, 2.5 compared with h/D=3.5

h/D	$Z'_{\dot{q}}$	Z'_{q}	$M'_{\dot{q}}$	M'_{q}
1.5	-14.80%	6.80%	9.92%	15.39%
2.5	-2.79%	2.06%	5.17%	14.49%

The test results show that the difference of hydrodynamic coefficients between h/D=2.5 and h/D=3.5 is small, and the difference between h/D=1.5 and h/D=3.5 is large, indicating that the depth has a great influence on the hydrodynamic coefficients of the MUV. From the longitudinal heading sailing test results, when the speed is 1.5-1.6 m/s, it is still subject to lift and trim moment pointing to the free surface. When the model is in heave and pitch motion, both the co-axial force and the orthogonal force can obtain a good linear relationship, but the pitch moment is a very small value, and the measured results are irregular, so it is necessary to measure multiple frequencies to find a linear relationship.

4. Conclusions

In this paper, some hydrodynamic coefficients near the free surface of the MUV model at different depths are measured by means of VPMM, including heading sailing test, horizontal oblique sailing test, heave and pitch motion test. Through the model test, the following conclusions can be obtained:

1) The resistance, vertical force and pitch moment measured by heading sailing test increase with the decrease of submergence depth, and the peak resistance appears when the inflow velocity U=1.4m/s.

2) Horizontal oblique sailing test results show that the free surface has little influence on the horizontal motion.

3) The values of vertical velocity, acceleration, angular velocity and angular acceleration are obtained by heave and pitch motion test, and the variation law with the depth is found.

The model test results shown in this paper provide the experimental verification for the numerical calculation of near-surface hydrodynamic forces of MUV, and also a reference for the simulation and control of near-surface maneuverability of MUV.

Acknowledgement

The authors want to thank the staff of the horizontal cycling tunnel laboratory and the support from the Key National Defense Laboratory of HEU for the experiments. They also thank the reviewers for their valuable comments.

R E F E R E N C E S

[1].*X. Jin*,"Prospects for the development and utilization of marine economy and the development in 21st Century",Scientific Chinese,**vol. 11**, 2006, pp. 13-17.

[2].*Y. Su, L. Wan, Y. Li, Y. Pang and Z. Qin*,"Development of a Small Autonomous Underwater Vehicle Controlled by Thrusters and Fins", ROBOT, **vol. 29**, no.2, 2007, pp.151-154.

[3].*Y. Xu, Y. Pang, Y. Gan and Y. Sun*,"AUV—state-of-the-art and prospect", CAAI Transactions o n Intelligent Systems,**vol. 1**, no. 1, 2006, pp.9-16.

[4]. *X. Yu, Y. Su, Z. Wang and L. Yang*,"Numerical Simulation of the Resistance of the MUV", Conference of Ship Hydrodynamics 2008,**vol. 11**, 2008, pp. 126-130.

[5]. *L. Zhang, L. Cheng, F. Li, Q. Sheng andY. Wang*, "Experiment on hydrodynamic interaction between 2D oval and wall", Journal of ship Mechanics,**vol. 10**, no.6, 2006, pp.1-10.

[6].*G. Li and W. Duan*,"Experimental study on the hydrodynamic property of a complex submersible", Journal of Ship Mechanics,**vol. 15**, no. 1-2, 2011, pp. 58-65.

[7]. *J. Zhu, Q. Chen, J. Gao and K. Huang*,"On the hydrodynamic forces of submersible with aerofoil section in forward and backward motions", JOURNAL OF HYDRODYNAMICS,**vol. 19**, no. 3, 2004, pp. 401-406.

[8]. *L. Yang, Y. Pang, L. Huang and A. Zhang*,"Study of the CFD approach to simulate PMM experiments of submarine", SHIP SCIENCE AND TECHNOLOGY, **vol. 31**, no. 12, 2009, pp. 12-17.

[9]. *X. Qi , A. Miao , D. WAN,*"CFD calculation of hydrodynamic derivatives of underwater vehicle", CHINESE JOURNAL OF HYDRODYNAMICS, **vol. 33**, no. 3, 2018, pp. 297-304.

[10]. *Kolodziejczyk W.*"The method of determination of transient hydrodynamic coefficients for a single DOF underwater manipulator",Ocean Engineering, **vol. 153**, no. 4, 2018, pp. 122-131.

[11]. *Juan Julca Avila, Kazuo Nishimoto, Claudio Mueller Sampaio, Julio C. Adamowski*,"Experimental Investigation of the Hydrodynamic Coefficients of a Remotely Operated Vehicle Using a Planar Motion Mechanism", Journal of Offshore Mechanics and Arctic Enfineering, **vol. 134**, no. 5, 2012, pp. 1-6.

[12]. *W. Chang*,"The Analysis and Research of Vertical Planar Motion Mechanism", A Dissertation for the Degree of M. Eng,**vol. 2**, 2005, pp. 35-43.